Basic Res Cardiol 96: 237 – 250 (2001)

ORIGINAL CONTRIBUTION

Josef Gehrmann
Stefan Frantz
Colin T. Maguire
Marcel Vargas
Anique Ducharme
Hiroko Wakimoto
Richard T. Lee
Charles I. Berul

Electrophysiological characterization of murine myocardial ischemia and infarction

Received: 5 October 2000
Returned for 1. revision: 2 November 2000
1. Revision received: 24 November 2000
Returned for 2. revision: 28 November 2000
2. Revision received: 13 December 2000
Accepted: 14 December 2000

J. Gehrmann · C. T. Maguire · M. Vargas
H. Wakimoto · Charles I. Berul, MD (✉)
Department of Cardiology
Children's Hospital · Boston
300 Longwood Avenue
Boston, MA 02115, USA
E-mail: berul@cardio.tch.harvard.edu

S. Frantz · A. Ducharme · R. T. Lee
Department of Cardiology
Brigham & Women's Hospital
Department of Medicine
Harvard Medical School
Boston, MA 02115, USA

Abstract *Background* Genetically altered mice will provide important insights into a wide variety of processes in cardiovascular physiology underlying myocardial infarction (MI). Comprehensive and accurate analyses of cardiac function in murine models require implementation of the most appropriate techniques and experimental protocols. *Objective* In this study we present in vivo, whole-animal techniques and experimental protocols for detailed electrophysiological characterization in a mouse model of myocardial ischemia and infarction. *Methods* FVB mice underwent open-chest surgery for ligation of the left anterior descending coronary artery or sham-operation. By means of echocardiographic imaging, electrocardiography, intracardiac electrophysiology study, and conscious telemetric ECG recording for heart rate variability (HRV) analysis, we evaluated ischemic and post-infarct cardiovascular morphology and function in mice. *Results* Coronary artery ligation resulted in antero-apical infarction of the left ventricular wall. MI mice showed decreased cardiac function by echocardiography, infarct-typical pattern on ECG, and increased arrhythmia vulnerability during electrophysiological study. Electrophysiological properties were determined comprehensively, but were not altered significantly as a consequence of MI. Autonomic nervous system function, measured by indices of HRV, did not appear altered in mice during ischemia or infarction. *Conclusions* Cardiac conduction, refractoriness, and heart rate variability appear to remain preserved in a murine model of myocardial ischemia and infarction. Myocardial infarction may increase vulnerability to inducible ventricular tachycardia and atrial fibrillation, similarly to EPS findings in humans. These data may be of value as a reference for comparison with mutant murine models necessitating ischemia or scar to elicit an identifiable phenotype. The limitations of directly extrapolating murine cardiac electrophysiology data to conditions in humans need to be considered.

Key words Myocardial infarction – mice – echocardiography – electrophysiology – heart rate variability

BRC 264

Introduction

Cardiac arrhythmias following ischemia and myocardial infarction (MI) may arise as a result of the progressive process of post-infarct tissue remodeling that may alter the substrate for electrical excitation and conduction. Clinical trials and experimental studies studying ventricular arrhythmias and mortality after MI in different species, such as the dog (11, 35, 75), pig (19, 69), rabbit (65), and rat (2, 36, 56) have contributed to the understanding of the mechanisms underlying arrhythmogenesis and to the development of diagnostic and therapeutic strategies. The rat model of MI has also been used in studies of ventricular remodeling (21, 63). As the mechanisms of electrical responses following MI are not fully understood, the availability of non-genetic murine models of infarction (42, 46, 51), ischemia and reperfusion (53+), and the development of genetic mouse models with altered expression of molecules that affect the ischemic process should yield insights into remodeling and arrhythmogenesis. For example, the recent generation of mice expressing disrupted, nonfunctional angiotensin II type 1 (33) and type 2 (27, 32), transgenic mice overexpressing heatshock protein (31), as well as mice overexpressing genes encoding the β_2-adrenergic receptor (54) and β-adrenergic receptor kinase (40) provide interesting genotypes. Recently, Yoshida, et al. (81) demonstrated that manipulation in the Sod I gene is responsible for the heart's vulnerability to ischemia reperfusion injury, and Sumeray (76) reported on the protective role of endothelial nitric oxide synthase (eNOS) against ischemia-reperfusion injury in a knockout mouse model. The recognition of the genetic and molecular bases of arrhythmogenic disorders will have an impact on clinical management (64), however phenotypic characterization is lagging behind the abilities to manipulate the genotype. Therefore, application of appropriate experimental methodology for functional analyses of the molecular mechanisms underlying resultant phenotypes is imperative. Technical limitations previously precluded accurate in vivo analysis of cardiovascular morphology, function, and electrophysiology in murine disease models. Analysis of integrated cardiovascular function in genetically engineered mice has been accomplished by miniaturization and refinement of methodologies used in larger mammals. To this end, we, as others (22, 28, 77), used transthoracic echocardiography for assessing changes of LV geometry and contractile function after experimental MI. To enhance our understanding of the fundamental mechanisms underlying cardiac conduction system function, we recently developed and described two novel techniques and protocols for electrophysiologic phenotyping in the mouse. The in vivo cardiac electrophysiology study allows comprehensive analysis of cardiac conduction and EP evaluation, including response to pacing, programmed stimulation, and pharmacological agents (7, 24).

In humans, decreased heart rate variability (HRV) is an independent predictor of increased morbidity and mortality with various forms of heart disease including myocardial infarction (10, 72). HRV analysis technology permits assessment of autonomic regulation of the murine heart rate in the conscious state and its potential contribution to arrhythmogenesis (25). The purpose of this study was to evaluate the electrophysiological properties of the murine conduction system, including influences of the autonomic nervous system on heart rate dynamics, and their correlation to structural changes in the context of remodeling after experimental ischemia and infarction.

Methods

Study animals

Adult male FVB mice, age 12–16 weeks (weight 20–29 g), were studied. Animals were randomly divided into either the MI groups (n = 16) and sham-operation control groups (n = 5). After completion of the functional studies, the heart was excised and presence or absence of MI was judged by gross macroscopic inspection. All protocols fully conformed to the Guide for the Care and Use of Laboratory Animals (NIH Pub. 85–23, 1996), Harvard Medical School and Children's Hospital Animal Care and Use Committees.

Coronary artery ligation

Sixteen mice underwent coronary artery ligation to induce a myocardial infarction. The details of the surgical procedure employed have been described elsewhere (53, 71, 83). Briefly, animals were anesthetized with pentobarbital, intubated, and ventilated. After opening the thoracic cavity, ligation of the left descending coronary artery was performed with a 7–0 silk suture, 3–4 mm from the tip of the left atrium. Each MI was confirmed by the following criteria: a) inspection immediately after LAD ligation in situ (paleness of left anterior ventricular myocardium), b) echocardiographic evidence of MI, c) macroscopic signs of MI at autopsy at the end of the study. All mice with ligation fulfilled these criteria and made up the MI-group. Mice assigned to the sham-operation group were subjected to the same procedure except the LAD was not ligated. The perioperative mortality was 37.5 % in MI mice and zero in sham-operated mice.

Echocardiography

Echocardiographic studies were performed 24 h after the surgical procedure under light anesthesia with spontaneous respiration using intraperitoneal tribromoethanol/amylene hydrate (Avertin) 2.5 % w/v solution (8 µl/g) (71). Imaging was performed by an ultrasonographer experienced in rodent imaging, using a Sonos 5500 (Hewlett Packard Medical; Andover, MA) and an 8–12 MHz transducer. A dynamically focused annular array and fusion frequency technology were employed, allowing ultrasound frequencies of up to 18 MHz. A standoff was used with the depth set at 4 cm with zoom mode to optimize resolution and penetration. Short-axis 2-dimensional echocardiographic images acquired at the mid-papillary and apical levels of the left ventricle were stored as digital loops. Frame acquisition rates using the loop mode reached 120 MHz, allowing excellent temporal resolution for 2-dimensional analysis. At the same anatomic levels, short-axis M-mode images were obtained at a sweep speed of 100 mm/s. Ultrasound analyses were performed by two researchers experienced in rodent echocardiography, neither of whom knew the surgical procedure performed in each animal. From M-mode short axis imaging, end-diastolic diameter, end-systolic diameter and fractional shortening [(end-diastolic diameter – end-systolic diameter)/end-diastolic diameter] were calculated. For each data point, three consecutive cardiac cycles were traced and averaged.

Electrocardiography and electrophysiology studies

The *in vivo* mouse cardiac electrophysiological study methodology has been previously described in detail (5–8). Briefly, mice were anesthetized by intraperitoneal administration of pentobarbital (0.033 mg/g). A tracheotomy was performed (7) and intubation was achieved for mechanical ventilation ($Fi_{O2} = 0.21$, $V_T = 1$cc, respiratory rate 130/minute). The surface frontal plane 6-lead ECG was obtained from 25 gauge electrodes placed subcutaneously in each limb and filtered between 0.5 and 250 Hz. ECG intervals (PR, QRS, QT, QTc) were calculated for each animal, and QT intervals were rate corrected using the formula proposed by Mitchell, et al. (55). For the EP study, conducted one week after coronary artery ligation, an octapolar 1.7 F catheter (CIBer mouse EP, NuMed, Inc., Hopkinton, NY) was inserted via jugular vein cutdown approach and placed into the right ventricle. Simultaneous atrial and ventricular pacing and recording were performed. Intracardiac ECGs were amplified (0.1 mV/cm) and filtered between 40 and 400 Hz, at an acquisition rate of 1000 samples/second. Standardized pacing protocols were used to determine the electrophysiological parameters, including sinus node recovery times, atrial, A-V nodal, and ventricular conduction properties and refractory periods (7). Each mouse underwent an identical pacing and programmed stimulation protocol. The stimulation protocol for arrhythmia induction consisted of programmed right atrial and right ventricular double and triple extrastimulation techniques down to a minimum coupling interval of 10 ms at 150-ms drive cycle length. Right atrial and right ventricular burst pacing with application of short bursts at rates of 30–50 ms for 1 min duration was also performed. The following definitions were used: negative study – no ventricular beats or up to four repetitive ventricular responses; nonsustained VT – five or more ventricular beats up to 30 s; sustained VT – VT lasting more than 30 s.

Heart rate variability (HRV) analysis

Animal preparation and surgery

For ambulatory, long-term ECG analysis, telemetry devices [Model TA10-F20, DataSciences Intl, St. Paul, MN] were implanted. Mice were anesthetized and the radiofrequency transmitter was inserted into a subcutaneous tissue pocket on the back.

Study protocol

Serial assessments of 60-minute ECG recordings were performed twice on the day of instrumentation at 1 hour and 3 hours, and on day 1, 4, and 14 after coronary artery ligation. Data was obtained from freely moving conscious mice between 9:00 AM and 3:00 PM.

Data acquisition and analysis

ECG signals were recorded using a telemetry receiver [DataSciences Intl, St. Paul, MN] and an analog-to-digital conversion data acquisition system [MacLab System, AD Instruments, Milford, MA]. The analog signal was digitized with 12-bit precision at a sampling rate of 2 kHz. ECG interval [PR, QRS, QT] measurements and calculations [QTc] were performed independently by two experienced investigators, blinded to the surgical procedure. Digital signal processing was performed using customized software written in the MATLAB [The Math Works, Inc, Natick, MA] programming language (25). A 120-s segment of the digitized ECG signal was digitally bandpass filtered [4–140 Hz], and the event detected using a threshold-lockout algorithm. For standardization, only stable segments of sinus rhythm were used for analysis. A graphical interface allowed visual reviewing and manual editing of erroneously detected events and aberrant ECG complexes, such as premature ventricular beats, electrical noise, or other errant ECG signals, and their adjacent RR intervals were excluded from analysis. The sequence of inter-event times was linearly interpo-

lated to a 20 Hz time series of beat intervals. HRV was quantified using standard time- and frequency-domain techniques (78). Adjacent 120-s signal epochs recorded during given test conditions exhibited comparable HRV metrics, obviating the need for joint time-frequency methods, such as a Wigner-Ville distribution, often applied to non-stationary signals (52).

Time-domain measures

Mean RR interval [RR_{mean}], median RR interval [RR_{median}], standard deviation (SD) of all normal RR intervals [SDNN], SD of averages of normal RR intervals [SDANN], and the square root of the mean of squared differences between adjacent normal RR intervals [RMSSD] were calculated directly from the sequence of inter-event times. Mean heart rate [HR_{mean}] was calculated as the mean of the sequence of the reciprocals of the inter-event times. As heart rate changes per se may affect HRV, an additional parameter was calculated to normalize the data for heart rate: the coefficient of variance [CV], defined as the SD of RR intervals/RR_{mean}.

Frequency-domain measures

Power spectral density of the beat-interval-time-series was computed using a modified averaged periodogram method. Specifically, the signal was divided into 12 overlapping segments of 512 samples. Each segment was mean-detrended, multiplied by a Hanning window and zero-padded to 1024 samples. The squared magnitudes of the discrete Fourier transform of the segments were averaged to form the power spectral density. Four different frequency-domain measures of heart rate variability were computed. Cutoff frequencies for power in the low-frequency range [LF] and high-frequency range [HF] and very low-frequency [VLF] were based on those utilized in human studies multiplied by a factor of 10 for heart rate adjustment [the approximate ratio between murine and human HR], and defined as 0.4 to 1.5 Hz, 1.5 to 4 Hz and 0.00 to 0.4 Hz respectively; total power [TP] was defined as 0.00 to 4 Hz. LF and HF were also measured in normalized units [nLF, nHF], representing the relative value of each power component in proportion to the sum of the HF and LF components (25, 59).

Statistical analysis

All statistical analyses were performed with Excel and STATA software. Values are presented as the mean ± 1 standard error of mean (SEM). Surface ECG and intracardiac conduction parameters were measured by two independent observers and compiled for statistical interpretation. Differences between groups were tested using a 2-tailed Student's t-test, analysis of variance (ANOVA) or chi-square distribution test, where appropriate. A 2-tailed t-test was used in comparisons of electrophysiologic data before and after myocardial infarction. A p value of < 0.05 was considered significant.

Results

Procedures and mortality

Ten MI mice (out of 16) and all 5 sham-operated mice survived throughout the study, for an overall survival rate of 72 %. Of the 6 animals that died, 2 died during coronary artery ligation, another 2 animals within 48 hours after surgery (echocardiographic and postmortem findings of large infarct, cardiac dilatation, LV rupture) and 2 mice died during the electrophysiologic study, due to anesthesia intolerance in one and atrial perforation in another. The mean age at surgery was 14.9 ± 2 weeks in the MI mice and 15.4 ± 2 weeks in sham-operated mice (p = NS). The mean weight at surgery was 23.7 ± 3 grams in the MI mice and 28.0 ± 3 grams in sham-operated mice (p = NS).

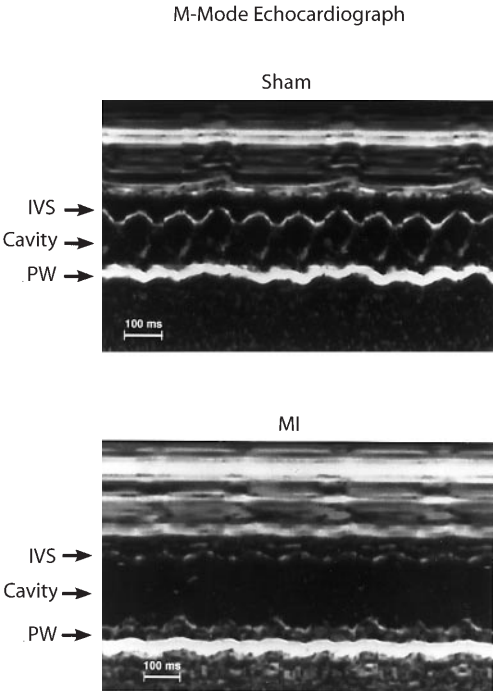

Fig. 1 Echocardiograms. Representative M-mode echocardiogram from a sham-operated (top) and a myocardial infarction (MI) mouse (bottom). Images were taken from a short axis view at the apical level. *IVS* interventricular septum; *PW* left ventricular posterior wall. Left ventricular cavity dilation and decreased shortening fraction is evident in the MI mouse.

Table 1 Summary of echocardiographic studies; means ± SEM

Echocardiographic parameters	Sham-operation (n = 5)	Myocardial infarction (n = 10)	p
Mid-papillary measurements			
ED diameter (mm)	2.5 ± 0.12	2.63 ± 0.19	0.86
ES diameter (mm)	0.8 ± 0.09	1.18 ± 0.16	0.19
FS (%)	69.0 ± 2.3	56.3 ± 3.7	0.06
Apical measurements			
ED diameter (mm)	1.95 ± 0.12	2.77 ± 0.16	0.004
ES diameter (mm)	0.33 ± 0.09	1.24 ± 0.17	0.002
FS (%)	81.5 ± 6.1	55.9 ± 5.0	0.007

Baseline echocardiographic measurements.
ED end diastolic; *ES* end systolic; *FS* fractional shortening

Effects of ischemia and myocardial infarction on morphological and functional parameters

Echocardiography was performed on the surviving 10 MI mice and 5 sham-operated mice 24 hours after surgery (Fig. 1). Myocardial infarction was defined by wall motion abnormalities (Table 1). The infarcted animals showed significantly increased chamber diameters at the apical level as compared with sham-operated animals; the end-diastolic diameters were 2.77 ± 0.16 versus 1.95 ± 0.12 mm, p = 0.004, the end-systolic diameters 1.24 ± 0.17 versus 0.33 ± 0.09 mm, $p = 0.002$. Mid-papillary measurements did not yield statistically significant differences between groups. Fractional shortening was significantly reduced (81.5 ± 6.1 % versus 55.9 ± 5.0 %, sham versus MI, $p = 0.007$). This reflects wall motion abnormalities in the infarcted area and early infarct expansion. Consistent with these early apical changes, the uninfarcted left ventricular myocardium, reflected in the papillary measurements, showed only non-significant signs of left ventricular enlargement.

In two sham-operated mice, transient repolarization abnormalities were noted on ECG perioperatively characterized by ST segment depression and T wave inversion consistent with ischemic myocardial injury. These mice exhibited no echocardiographic alterations and absence of MI was demonstrated later by pathologic examination.

Effects of ischemia and myocardial infarction on the murine cardiac electrophysiology

A total of 15 of 21 mice (71 %) were evaluated with the mouse EP study protocol. Full 6-lead ECG data were obtained on 19 mice (90 %) and right jugular venous access was successfully obtained on 17 mice (81 %). Complete electrophysiological data were obtained from 10 of 16 mice that underwent left anterior descending coronary artery ligation.

Electrocardiographic data

ECG measurements and calculations for all animals studied are summarized in Table 2. The average resting sinus cycle length (SCL) was significantly faster in myocardial infarction mice (126.5 ± 19.9 ms) compared to sham-operated mice (173.9 ± 61.6 ms), $p = 0.02$, at 3 hours post infarction. No statistical significant differences were observed in PR, QRS, QT, and QTc intervals at any time point post infarction chosen in this series. The surface ECG recordings proved to be a very useful tool in determining the operative procedure of ligating the coronary artery versus doing a sham procedure. 100 % (14 of 14) of the animals that developed myocardial infarction, as proven later by echocardiography and gross pathological examination, exhibited a strikingly pathologic, infarct-typical ECG pattern during and after the operative procedure, compared to 0 of 5 sham-operated group (Table 3). The pathologic ECG pattern persisted over the entire study period. The early ECG manifestations of transmural MI included a diminished R wave amplitude, marked ST segment elevation and the development of a significant Q wave. A representative surface ECG from a

Table 2 Summary of electrocardiographic parameters; means ± SEM

ECG parameters	Time after operation					
	Sham-operation (n = 5 each)			Myocardial infarction (n = 10 each)		
	3 hours	day 4	day 14	3 hours	day 4	day 14
SCL (ms)	173.9 ± 61.6*	80.0 ± 3.5	78 ± 2	126.5 ± 19.9	84.2 ± 8.6	80.9 ± 4.6
PR (ms)	41.5 ± 12.9	25.7 ± 1.7	26.5 ± 1.0	37.9 ± 6.1	25.4 ± 1.8	26.2 ± 2.9
QRS (ms)	18.0 ± 3.0	13.3 ± 0.7	12.6 ± 1.2	18.7 ± 5.3	12.9 ± 0.7	12.1 ± 1.2
QT (ms)	78.9 ± 26.3	47.9 ± 3.2	47.4 ± 4.2	67.2 ± 10.1	52.1 ± 5.2	46.1 ± 3.2
QTc (ms)	60.0 ± 11.6	53.6 ± 3.7	53.7 ± 3.9	59.7 ± 5.3	56.8 ± 4.4	51.3 ± 3.3

Abbreviations: *SCL* sinus cycle length, *PR* PR interval, *QRS* duration of the QRS complex, *QT* QT interval, *QTc* corrected QT interval. *P < 0.05 sham-operation vs. myocardial infarction

Table 3 Myocardial infarct detection

	ECG		Echo	Pathology
	Deep Q Wave	ST Segment Elevation		
Sham-operation (n = 5)	0/5 (0 %)	0/5 (0 %)	0/5 (0 %)	0/5 (0 %)
Myocardial infarction (n = 10)	10/10 (100 %)	10/10 (100 %)	10/10 (100 %)	10 /10 (100 %)

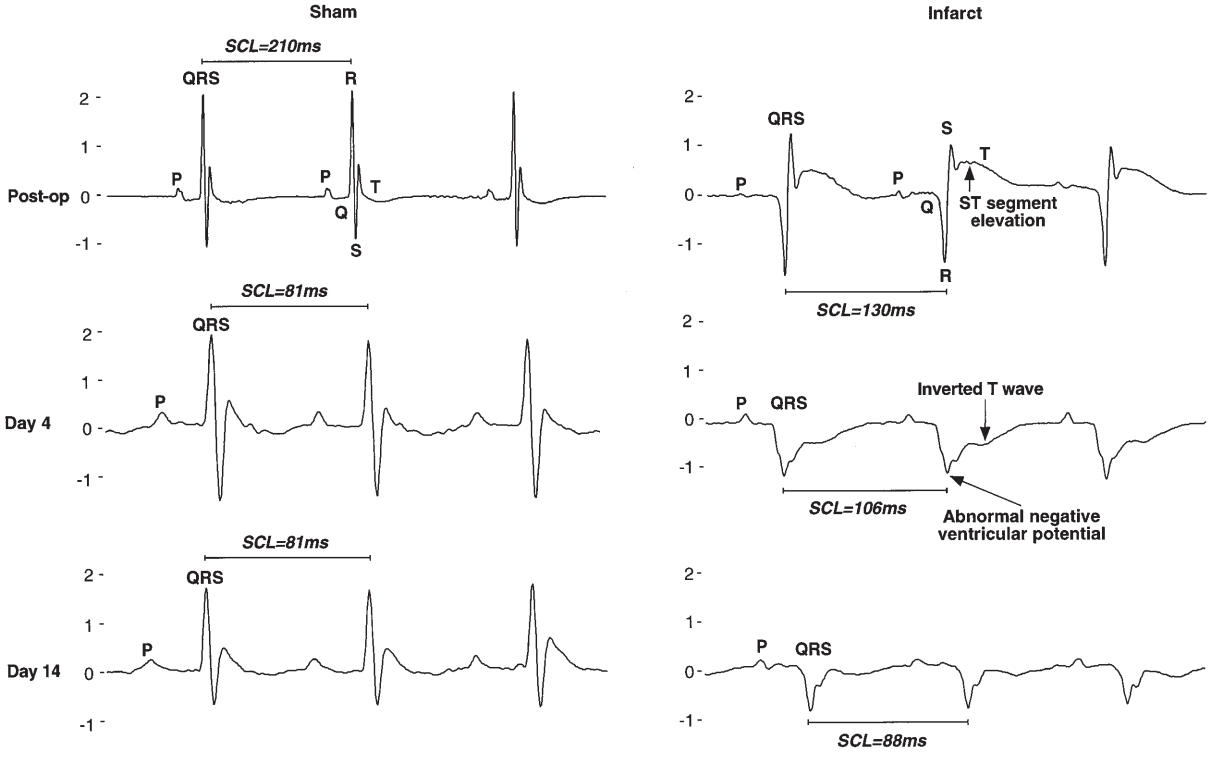

Fig. 2 Electrocardiograms. Surface electrocardiogram (ECG) from sham-operated mouse (left) and infarcted mouse (right). The ECG was recorded at 1 hour post-operatively (top), day 4 (middle) and day 14 (bottom) following surgery. The P waves, QRS, and T waves are visible and annotated, and the sweep speed is normalized for sinus cycle length (SCL) for comparisons. The SCL is shorter acutely post-operatively in MI mice, and recovers to normal by 4 days post-operatively. Following infarct, there is acute ST segment elevation, followed by development of chronic negative "Q" waves.

mouse during the acute ischemic and chronic phase after coronary artery ligation is shown in Fig. 2. The infarct-typical ECG pattern was easily distinguishable from the transient phenomena relating to ischemia observed in a subset of sham-operated mice (see above).

Cardiac conduction properties and electrophysiologic study

Atrial, A-V, and ventricular conduction properties were assessed in sham-operated and MI mice. The mean ± SD sinus cycle lengths were 188.5 ± 19.8 ms in sham-operated mice, equivalent to an average of 318 ± 32 bpm, and 227.0 ± 33.4 ms in the MI mouse group, corresponding to a heart rate of 264 ± 43 bpm.

The electrophysiological parameters obtained are displayed in detail in Table 4. Sinus node function, evaluated by indirect measurement of SNRT, exhibited no significant differences between groups. AV conduction remained intact with atrial pacing down to an average paced cycle length of 110.0 ± 9.1 ms (545 bpm) in the sham-operated mice compared to 116.2 ± 12.4 ms (516 bpm) in the MI mice. Pacing at more rapid rates caused AV-His-Purkinje system block. The maximum cycle length that produced 2:1 AV block was 88.7 ± 7.5 ms (676 bpm) in the sham group and 96.2 ± 11.9 ms (624 bpm) in the MI group. Higher-grade AV block was not observed in any of the mice. With programmed atrial stimulation with single and double atrial premature extrastimuli at two pacing drive rates, the mean AVERP was 71.3 ± 8.5 ms in sham-operated mice versus 90.0 ± 11.9 ms in MI mice with pacing at 200-ms cycles (p = 0.02), and 76.2 ±

Table 4 Summary of electrophysiological studies

	Sham-operation (n = 5)	Myocardial infarction (n = 10)	P
Atrial pacing parameters			
Threshold	0.1 ± 0.0	0.11 ± 0.03	0.5
Sinus node			
Sinus cycle length (SCL)	188.5 ± 19.8	227.0 ± 33.4	0.16
$SNRT_{200}$	246.3 ± 40.9	292.7 ± 39.2	0.11
$CSNRT_{200}$	57.8 ± 43.7	65.7 ± 45.8	0.85
$SNRT/SCL_{200}$ %	131.4 ± 23.6	131.3 ± 24.9	0.95
$SNRT_{150}$	299.8 ± 42.7	327.0 ± 69.0	0.71
$CSNRT_{150}$	86.3 ± 33.2	98.9 ± 53.5	0.69
$SNRT/SCL_{150}$ %	141.6 ± 15.1	144.5 ± 27.1	0.70
$SNRT_{100}$	354.0 ± 48.5	338.6 ± 64.2	0.39
$CSNRT_{100}$	138.3 ± 33.5	109.2 ± 53.5	0.38
$SNRT/SCL_{100}$ %	164.4 ± 14.4	149.4 ± 26.6	0.51
A-V node			
AV interval	42.2 ± 2.1	42.7 ± 4.6	0.55
AVC (min CL)	110.0 ± 9.1	116.2 ± 12.4	0.19
AV Wenckebach	105.0 ± 9.1	111.2 ± 12.4	0.79
AV 2:1	88.7 ± 7.5	96.2 ± 11.9	0.87
$AVERP_{200}$	71.3 ± 8.5	90.0 ± 11.9	0.02
$AVERP_{150}$	76.2 ± 7.5	88.1 ± 15.1	0.17
Ventricular pacing parameters			
Threshold	0.15 ± 0.1	0.29 ± 0.23	0.27
VAC (min CL)	135.0 ± 25.9	168.3 ± 37.5	0.27
VA Wenckebach	130.0 ± 25.9	163.3 ± 37.5	0.27
VA 2:1	98.3 ± 30.1	107.5 ± 3.5	0.71
$VERP_{200}$	35.0 ± 9.1	32.1 ± 12.2	0.69
$VERP_{150}$	37.5 ± 9.6	41.9 ± 20.0	0.69

Values are means ± SEM, with intervals in milliseconds, unless other indicated. *Threshold* minimum pacing threshold (milliamperes at 1.0-ms pulse duration). *SCL* sinus cycle length; *SNRT* sinus node recovery time; *CSNRT* corrected SNRT (SNRT-SCL); *AV* atrio-ventricular; *AV Wenckebach* atrial pacing Wenckebach cycle length; *AV 2:1* atrial pacing 2:1 AV block cycle length; *VA* ventriculo-atrial; *ERP* effective refractory period; "200", "150" and "100" refer to the cycle lengths (in ms) of the pacing protocols. *VAC (min CL)* VA conduction minimum cycle length; *VA Wenckebach* ventricular paced maximum cycle length allowing VA conduction; *VA 2:1* ventricular paced maximum cycle length causing 2:1 VA block; *VERP* ventricular ERP

7.5 versus 88.1 ± 15.1 ms respectively at 150-ms cycles (p = 0.17). Ventricular pacing demonstrated retrograde VA conduction in 3 of 5 (60 %) sham-operated mice and 6 of 10 (60 %) MI mice. In those animals showing intact retrograde VA conduction, the conduction remained intact to a minimum paced ventricular cycle length of 135.0 ± 25.9 ms in the sham-operated mice compared to 168.3 ± 37.5 ms in the MI mice, which are similar to the antegrade block rates (antegrade versus retrograde conduction, *p* = NS).

Table 5 Arrhythmia inducibility

	Atrial pacing protocols		Ventricular pacing protocols	
	A Fib	NSVT	A Fib	NSVT
Sham-operated (n = 5)	0/5 (0 %)	0/5 (0 %)	0/5 (0 %)	1/5 (20 %)
Myocardial infarction (n = 9)	3/9 (33 %)	0/9 (0 %)	1/9 (11 %)	6/9 (67 %)

A Fib Atrial fibrillation; *NSVT* Non-sustained ventricular tachycardia

Programmed electrical stimulation and arrhythmia inducibility

Using standard programmed electrical stimulation protocols and burst atrial and ventricular pacing, provocation of ectopic or reentrant rhythms was attempted. The vulnerability for arrhythmias is illustrated in Table 5. We defined a sustained arrhythmic episode as one that lasted > 30 s. Non-sustained ventricular tachycardia (0.5–29 s) was reproducibly inducible by single, double and triple premature ventricular extrastimuli or by burst ventricular pacing in 6 out of 9 (67 %) myocardial infarction mice. Additionally, atrial fibrillation (0.5–29 s) was inducible by burst atrial pacing or programmed atrial stimulation with single or double extrastimuli in 3 out of 9 (33 %) myocardial infarction mice. In one MI mouse (11 %), atrial fibrillation was also induced by ventricular burst pacing. Representative examples of the induced arrhythmias are illustrated in Fig. 3. In the sham-operated control group, non-sustained ventricular tachycardia was inducible only with burst ventricular pacing in 1 out of 5 (20 %) mice. Neither atrial nor ventricular stimulation protocols could provoke any atrial arrhythmias. We did not observe supraventricular tachycardias (SVT), sustained atrial fibrillation, sustained ventricular tachycardia, ventricular fibrillation, nor sudden cardiac death in any mouse.

In summary, comparing the two study groups, there were no significant differences between atrial and ventricular conduction properties and refractoriness. The EP study findings further provide strong evidence that arrhythmia vulnerability is markedly increased in both ventricle and atrium after experimental myocardial infarction in mice.

Effects of ischemia and myocardial infarction on measures of heart rate variability

Table 6a demonstrates the time-dependent course of heart rate dynamics in both study groups. During the ischemic phase (3 hours postoperatively), MI mice had faster heart rates (478 ± 57 bpm) compared to the sham-operated control group (360 ± 63 bpm), p = 0.02. On day

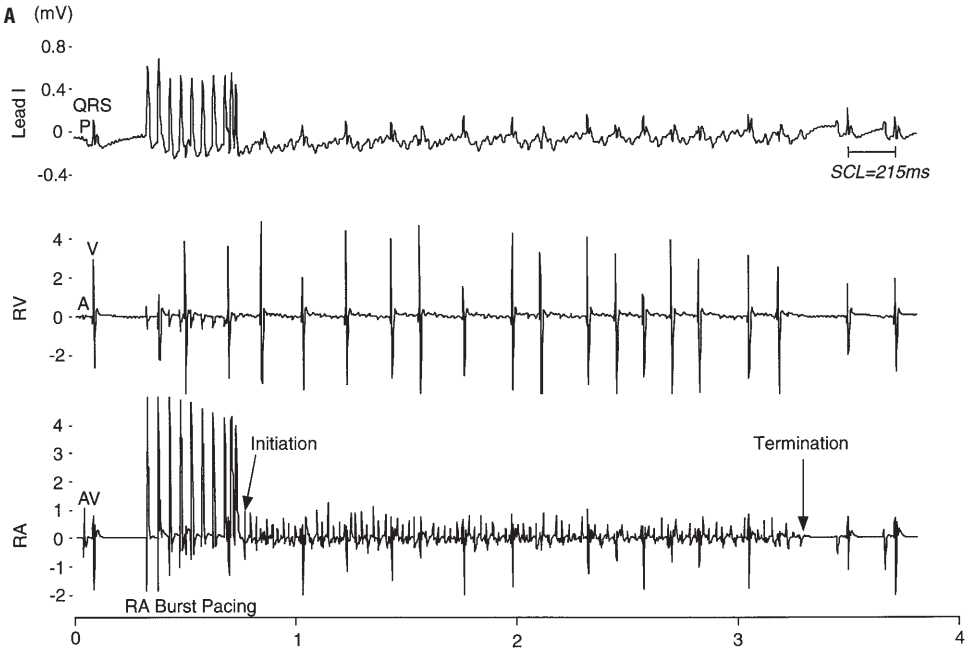

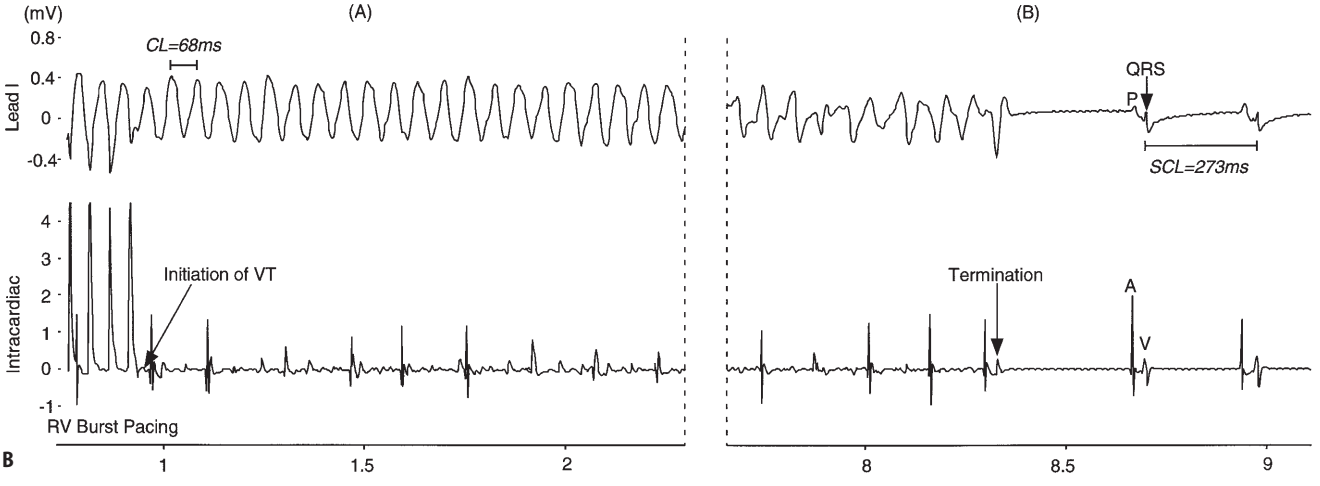

Fig. 3 Arrhythmia examples in MI mice. **A** Atrial tachycardia. The top panel is lead I of a surface electrocardiogram (ECG), middle panel is the right ventricular (RV) intracardiac electrogram, and lower panel is the right atrial (RA) electrogram. The first beat is sinus, with distinct P wave and QRS complex on ECG (and A and V spikes on intracardiac electrograms). Right atrial pacing is performed which initiates a rapid atrial tachycardia, with variable ventricular conduction, and spontaneously converts back to normal sinus rhythm. **B** Ventricular tachycardia. The top panel is ECG lead I, and the lower panel is a composite intracardiac electrogram. Burst pacing in the right ventricle (RV) initiates a monomorphic-appearing ventricular tachycardia (VT) at a cycle length (CL) of 68 ms. Ventriculo-atrial block is demonstrated on the intracardiac channel. The tachycardia degenerates into a polymorphic VT and then spontaneously terminates, with recovery of sinus rhythm.

Table 6a Time domain measures of heart rate variability; means ± SEM

Parameters of HRV	Time after operation									
	Sham-operation (n = 5 each)					Myocardial infarction (n = 10 each)				
	1 hour	3 hours	day 1	day 4	day 14	1 hour	3 hours	day 1	day 4	day 14
RR (ms)	178 ± 42	185 ± 21*	89 ± 11*	78 ± 4	78 ± 3	150 ± 39	127 ± 17	123 ± 35	84 ± 6	81 ± 1
HR (bpm)	370 ± 87	360 ± 63*	679 ± 77*	769 ± 44	772 ± 25	423 ± 99	478 ± 57	518 ± 130	719 ± 52	745 ± 9
SDNN (ms)	1.0 ± 0.7	1.2 ± 0.5	5.3 ± 3.1	2.4 ± 1.4	1.3 ± 0.6	1.4 ± 0.9	3.1 ± 1.9	7.0 ± 2.6	3.1 ± 1.5	1.9 ± 0.5
SDANN (ms)	0.6 ± 0.4	0.5 ± 0.2	3.3 ± 3.3	1.1 ± 1.1	0.6 ± 0.4	0.6 ± 0.4	0.9 ± 0.5	2.4 ± 1.5	1.1 ± 0.8	0.7 ± 0.3
CV (%)	0.6 ± 0.4	0.7 ± 0.3	5.9 ± 3.5	3.1 ± 1.8	1.0 ± 0.8	0.9 ± 0.6	0.7 ± 2.2	5.7 ± 2.1	3.7 ± 1.8	2.3 ± 0.6
RMSSD (ms)	1.7 ± 1.4	2.0 ± 0.8	4.7 ± 2.1	3.7 ± 2.0	1.7 ± 0.5	2.0 ± 0.8	6.0 ± 5.8	8.5 ± 5.2	4.0 ± 2.1	3.1 ± 1.6

Abbreviations: *RR* RR interval; *HR* heart rate, measured in beats per min (bpm); *SDNN* standard deviation of all normal RR intervals; *SDANN* standard deviation of the average RR interval; *CV* coefficient of variance; *RMSSD* the square root of the mean of the squared differences between adjacent normal RR intervals. *P < 0.05 sham-operation vs. myocardial infarction

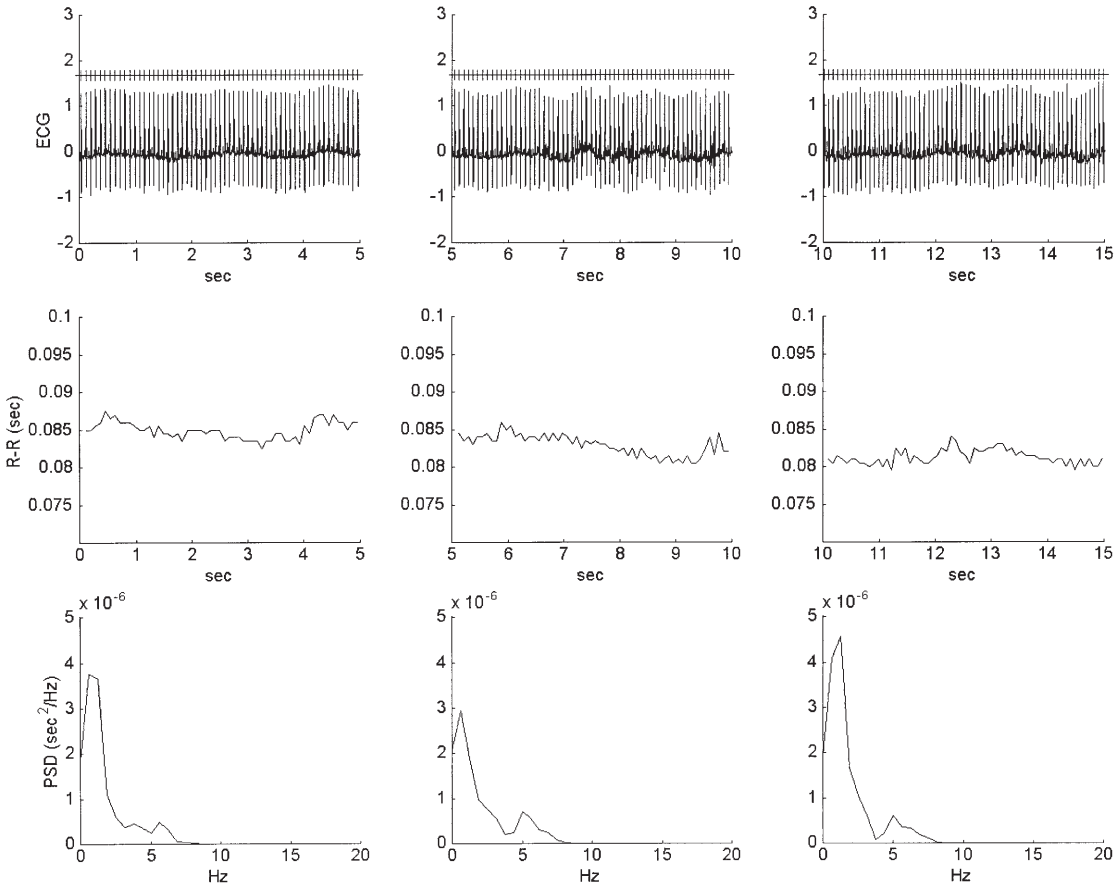

Fig. 4 Heart rate tachogram and spectral analysis of heart rate variability. The top three panels illustrate consecutive 5-s segments of ECG lead I telemetered recording from a myocardial infarction mouse. The detected beats are indicated by tick marks directly above the electrogram tracings. The middle panels show R-R intervals computed from detected ECG beats. The bottom panels reveal the power spectra computed from the R-R interval time series. The time series (40 Hz) were calculated from beat series using linear interpolation. Although plots of R-R intervals show low frequency (LF) oscillations, such biological noise is likely due to activity of the conscious, unrestrained animals. The similarity of spectral power traces over the three consecutive segments indicates stationarity of the signals.

1 following the surgical procedure, HR almost normalized in the sham-operated mice, whereas recovery of HR was incomplete in the MI mice. By postoperative day 4, in the phase of acute MI, and continuing until the end of the study period on day 14 ("infarct scar") normal values for heart rate were reached in all mice without any differences between groups (Fig. 4).

Table 6b Frequency domain measures of heart rate variability; means ± SEM

Parameters of HRV	Time after operation									
	Sham-operation (n = 5 each)					Myocardial infarction (n = 10 each)				
	1 hour	3 hours	day 1	day 4	day 14	1 hour	3 hours	day 1	day 4	day 14
Total power (ms^2/Hz)	12.1 ± 16.0	15.1 ± 14.9	382.7 ± 413.1	75.1 ± 78.1	19.1 ± 21.3	28.3 ± 48.1	109.2 ± 113.8	602.1 ± 430.2	114.1 ± 122.0	30.5 ± 14.4
LF power (ms^2/Hz)	3.0 ± 5.3	2.0 ± 1.7	52.0 ± 45.9	17.8 ± 17.1	3.4 ± 3.0	9.0 ± 18.2	28.5 ± 38.9	94.0 ± 129.2	14.1 ± 13.3	4.8 ± 2.9
HF power (ms^2/Hz)	0.7 ± 0.6	1.2 ± 1.5	20.4 ± 17.6	11.9 ± 6.1	1.5 ± 0.9	1.8 ± 1.7	23.5 ± 32.3	29.5 ± 22.4	9.1 ± 7.3	2.8 ± 0.8
VLF power (ms^2/Hz)	8.4 ± 10.3	11.1 ± 10.4	310.3 ± 354.6	55.5 ± 78.2	14.2 ± 17.8	17.6 ± 28.5	57.1 ± 53.0	478.5 ± 338.3	90.9 ± 104.4	22.9 ± 11.8
nLF power	0.81 ± 0.1	0.62 ± 0.2	0.71 ± 0.1	0.6 ± 0.2	0.69 ± 0.1	0.83 ± 0.3	0.45 ± 0.2	0.76 ± 0.1	0.6 ± 0.1	0.63 ± 0.2
nHF power	0.19 ± 0.1	0.38 ± 0.2	0.29 ± 0.1	0.4 ± 0.2	0.31 ± 0.1	0.17 ± 0.3	0.55 ± 0.2	0.24 ± 0.1	0.4 ± 0.1	0.37 ± 0.2
LF/HF ratio	4.2 ± 2.9	1.7 ± 1.0	2.7 ± 0.8	1.5 ± 1.2	2.3 ± 0.8	5.8 ± 2.7	1.2 ± 1.2	3.1 ± 1.9	1.5 ± 1.2	1.7 ± 0.5

Abbreviations: *LF* low-frequency; *HF* high-frequency; *VLF* very low frequency; *n* normalized

It is further evident that there were no significant changes in any of the time-and frequency-domain variables of the heart rate variability as a consequence of ischemia, acute myocardial infarction nor in the chronic phase of the "infarct scar". Table 6a illustrates the detailed data of all time-domain variables (SDNN, SDANN, CV, and RMSSD) which remain highly preserved over the entire study period. Table 6b shows that calculations of total power, LF power, HF power, and VLF power of frequency-domain variables did not reveal a reduction in total nor in the individual power of spectral components. The higher values for LF power compared to HF power, and the positive LF/HF ratio indicate a sympathetic predominance and a low vagal tone in all mice in both experimental groups. Particularly in the frequency-domain, HRV data showed a high inter-individual variation.

Discussion

Major advances in transgene and gene targeting technology have made the mouse the principal animal model for studying molecular mechanisms underlying disordered cardiac conduction and sudden cardiac death following myocardial ischemia or infarction. The main findings of this study can be summarized as follows: a) we confirmed prior demonstrations of the feasibility of coronary artery ligation for MI induction in mice as well as the echocardiographic visualization and quantification of the structural sequelae following MI, b) we determined the functional electrophysiological consequences of ischemia and infarction, including the propensity for arrhythmias, and c) we evaluated the impact of autonomic nervous system HR modulation by means of serial HRV analysis. To our knowledge, this is the first study in the mouse to describe the impact of myocardial ischemia and infarction on the cardiac conduction system *in vivo*, the role of the autonomic nervous system on heart rate dynamics, and to directly correlate structural echocardiographic parameters with functional electrophysiological measurements.

Cardiovascular research has focused attention on the electrophysiological architecture of ventricular myocardium in the ischemic and infarcted heart (45, 62, 66). Several lines of experimental evidence obtained in a canine model of myocardial infarction clearly demonstrated the impact of disturbed gap-junctional pattern in the healing epicardial border zone on impulse conduction and arrhythmogenesis (17, 30, 62). In humans, altered connexin43 gap junction distribution has been shown in the border zone of healed infarcts (74). Connexin43 knockout (67) and other transgenic mouse models are available and have recently been characterized electrophysiologically (26, 57). Mouse models of myocardial ischemia and infarction may be used to study the molecular mechanisms of myocardial stunning, preconditioning and the role of adhesion molecules in genetically altered mice (53).

Coronary artery ligation and animal model

Coronary artery ligation as a method to induce myocardial infarction has been extensively documented in rats (41, 63) and more recently, Michael, et al. (53) described mouse coronary artery anatomy and methods of coronary artery ligation. Lutgens, et al. (46) delineated the cardiac structural and functional consequences with respect to infarct localization, LV morphology, DNA synthesis and interstitial fibrosis. Patten, et al. (61) quantified hemodynamics and parameters of ventricular remodeling in a mouse model of MI. Coronary artery anatomy in the mouse is comparable to that of other mammals, with early branching of a septal artery from the left coronary system (18). It is well known that type and incidence of the electrical changes and arrhythmias differ among species. In larger species (dog, pig, cat), the arrhythmias following ischemia and infarction are relatively well characterized and whereas several observations provided circumstantial evidence that the electrical changes in humans and large animal hearts are similar, this may not be the case for small animals (16, 18, 34, 36). By miniaturization of instruments, technical limitations have recently been overcome and comprehensive functional analysis in mice is now feasible.

Echocardiography, left ventricular dysfunction and arrhythmia vulnerability in MI mice

In the present study, we provide confirmatory evidence that echocardiography is a reliable and non-invasive means to study LV dimensions and dysfunction after MI in mice. Wall motion abnormalities and increased chamber diameters were mainly seen apically. The echocardiographic studies were conducted in the acute phase after MI and results therefore represent early effects on left ventricular diameters. Others (22) reported on the use of serial echocardiographic assessment of LV dimensions and function after MI, which is important to define the time-dependent process of post-infarct remodeling. We also demonstrated that the echocardiographic parameters correlated well with ECG changes and arrhythmia vulnerability during EP study.

Electrocardiography and electrophysiology during ischemia and after myocardial infarction

The basic electrocardiographic time intervals (PR, QRS, QT, and QTc) were similar in both groups and in agree-

ment with those reported in earlier studies in mice (5–8). During the ischemic phase, MI mice had faster heart rates compared to the sham-operated controls. This may be caused by a more pronounced increase in sympathetic tone in these mice versus their sham-operated counterparts, or alternatively, may simply be a consequence of differential heart rate response to surgery and anesthesia. By day 4, full recovery of SCL time intervals was reached which remained constant over the 2-week follow-up period. Our *in vivo* murine EP methodology, based on analogous clinical protocols used to evaluate cardiac conduction in humans, allows a comprehensive assessment of the conduction characteristics relevant for understanding arrhythmia mechanisms. The major electrophysiological conclusions from this study are that myocardial infarction causes increased inducibility of ventricular and atrial arrhythmias. Electrophysiological properties did not significantly differ when compared to control mice. These findings are in good agreement with studies performed in other mammalian species (82) and closely reflect results obtained in human clinical studies. Therefore this approach validates the mouse as a model to assess post-MI arrhythmic risk stratification. The fundamental mechanisms of cardiac electrical activity at the molecular level involving gap junctions, membrane ion channels or other genetic manipulations underlying post-ischemic and post-infarction cardiac arrhythmias are now amenable to thorough investigation on the whole animal level.

Heart rate variability during ischemia and after myocardial infarction

There have been few basic reports of HRV analysis in smaller animals such as rats and mice (12, 43) and HRV analysis has been employed in transgenic mouse models (38, 52, 79, 80). However, as yet, few data are available on the influence of myocardial ischemia and infarction on autonomic innervation of the heart in mice. Depressed HRV is a powerful predictor of mortality and of arrhythmic complications, particularly sudden cardiac death, in patients after acute MI (39, 58). The underlying physiologic mechanism of decreased HRV is thought to reflect an alteration in cardiac sympathetic-parasympathetic balance, characterized by a relative sympathetic dominance likely secondary to reduced parasympathetic activity. It has been further proposed that this imbalance may lead to cardiac electrical instability (82). As the time after acute MI at which depressed HRV reaches the highest predictive value has not been fully investigated, and to ascertain the process of autonomic remodeling, we chose to perform serial assessments during ischemia and post MI. The surprising finding of the present study is that we did not demonstrate convincing evidence of measurable autonomic imbalance after myocardial infarction in mice. Contrary to our expectations, a significant decrease in HRV measured was not seen, either in the early ischemic period or in the chronic MI phase. The results obtained in the sham-operated and even the MI mice were similar to those we recently reported in a larger cohort (n = 24) of normal mice (25). These findings are in contrast to studies conducted in other species including humans (20, 39, 44), and rats (3, 41) demonstrating that HRV is depressed after MI. As this is the first study of this kind in mice, no data are available for comparison. Post-MI reduction of heart rate variability seen in different species is considered a reflection of increased sympathetic and reduced vagal activity (14, 41). How can our data of unaltered measures of HRV after MI in the mouse be interpreted in the light of the aforementioned evidence derived from different mammalian species? There are at least two possible answers to this question. First, the divergent findings in the mouse might be related to the study protocols, techniques or to the algorithms used; influenced by extrinsic factors rather than species-specific variables. This is unlikely, as we were recently able to demonstrate that analysis of beat-to-beat fluctuations in murine heart rate provides a quantitative measure of parasympathetic and sympathetic influences on heart rate modulation. We showed that responses to pharmacological manipulation are quantifiable, reproducible and qualitatively similar to those in larger mammals including humans (25). Second, it is conceivable that the mouse is indeed different from other species with respect to the sympatho-vagal makeup. We favor this latter hypothesis based on the following lines of evidence. In mice, sympathetic tone predominates (or vagal tone is low) under physiological conditions; in previous experiments of others (37, 52, 80) and our group neither parasympathetic blockade nor sympathetic stimulation was able to increase heart rate (25). High-frequency power is predominantly a marker of cardiac parasympathetic control (3), whereas low-frequency power receives both sympathetic and parasympathetic contributions, with a large parasympathetic component as shown in human (1, 4, 73) and canine studies (7, 13, 29, 68). We could fully confirm this phenomenon in mice (25). As vagal tone in mice is attenuated by the saturating influence on the sinus node of a persistently high sympathetic tone under physiologic conditions, vagal input withdrawal after MI may not at all be measurable by HRV analysis. According to the present data, the original proposition of increased sympathetic and reduced vagal activity after MI is not identifiable in the mouse. Our previous observation, that pharmacological parasympathetic blockade significantly reduced time- and frequency domain measures of HRV in normal mice, suggests that pharmacological intervention may be a more powerful means of vagal withdrawal than MI. With respect to sympathetic-induced electrical instability, the capability of time-and frequency domain measures of

HRV to predict total cardiac and arrhythmic mortality therefore seems to be of limited value in the mouse. In contrast to findings in humans (15, 50, 56, 70) and other species (82), in mice the genesis of arrhythmic events (see above) does not seem to be caused by myocardial autonomic denervation as there was no evidence of impaired autonomic function. This is further supported by the results obtained during EP study which showed no significant alterations in cardiac conduction and other electrophysiological properties (see above). In summary, these data may indicate a high degree of species-specific dissimilarity, suggesting that the mouse may not be optimally suited for the investigation of autonomic nervous system function and risk stratification during ischemia and post-myocardial infarction.

Limitations of the study

For potential general limitations of murine cardiac electrophysiology and HRV analysis we refer to the recent literature (24, 25). In the present study, we did not perform pharmacological blockade to study the frequency-specific contributions to HRV. All of the ECG recordings were obtained during daytime hours, and as mice are nocturnal animals, the most active phase of the circadian cycle was not assessed. During daytime recordings, however, appropriate grooming behaviors and physical activity were documented. In humans, a smaller day-night heart rate difference in addition to reduction in HRV and a tendency towards faster heart rates is thought to reflect autonomic imbalance after myocardial infarction. We did not observe spontaneous arrhythmias nor sudden death on ambulatory ECG, perhaps due to the relatively short duration of the ECG recordings. Short-term HRV recordings, as performed in this study, may provide less prognostic information for risk stratification after MI than from 24-hour recordings (9, 48). Finally, the relatively small sample size and wide variability in the sham group may weaken the statistical power, particularly for the HRV indices, although our prior work on HRV in control mice (25) may support the validity of the present findings. In conclusion, our studies provide background information for future investigations of cardiac morphology, conduction abnormalities, arrhythmogenicity, autonomic nervous system function, and post-myocardial infarct risk stratification in genetic mouse models of myocardial ischemia and infarction. We demonstrated the feasibility to address these questions using appropriate whole-animal, in vivo technology. However, the present study also underscores that experimental data obtained from the mouse cannot be directly extrapolated to conditions in humans in all aspects of cardiovascular pathophysiology.

Acknowledgments J. G. is supported by a grant from the University of Münster, Germany. S. F. is supported by a grant from the Deutsche Forschungsgemeinschaft. C.I.B. is supported in part by N.I.H. grants K08-HL-03607 and P50-HL-61036. We thank Peter Hammer and John Triedman, MD for their assistance with custom software for spectral analysis and critical review of the manuscript.

References

1. Ahmed MW, Kadish AH, Parker MA, Goldberger JJ (1995) Effect of physiologic and pharmacologic adrenergic stimulation on heart rate variability. J Am Coll Cardiol 24: 1082–1090
2. Aimond F, Alvarez JL, Rauzier JM, Lorente P, Vassort G (1999) Ionic basis of ventricular arrhythmias in remodeled rat heart during long-term myocardial infarction. Cardiovasc Res 42: 402–415
3. Akselrod S, Gordon D, Vbel FA, Shannon DC, Barger AC, Cohen RJ (1981) Power spectrum analysis of heart rate fluctuation. Science 213: 220–222
4. Arai Y, Saul JP, Albrecht P, Hartley HL, Lilly LS, Cohen RJ, Calucci WS (1989) Modulation of cardiac autonomic activity during and immediately after exercise. Am J Physiol 256: H132–141
5. Berul CI, Maguire CT, Aronovitz MJ, Greenwood J, Miller C, Gehrmann J, Housman D, Mendelsohn ME, Reddy S (1999) DMPK dosage alterations result in atrioventricular conduction abnormalities in a mouse myotonic dystrophy model. J Clin Invest 103: R1–R7
6. Berul CI, Christe ME, Aronovitz MJ, Seidman CE, Seidman JG, Mendelsohn ME (1997) Electrophysiological abnormalities and arrhythmias in a-MHC mutant familial hypertrophic cardiomyopathy mice. J Clin Invest 99: 570–576
7. Berul CI, Aronovitz MJ, Wang PJ, Mendelsohn ME (1996) In vivo cardiac electrophysiology studies in the mouse. Circulation 94: 2641–2648
8. Bevilacqua LM, Simon AM, Maguire CT, Gehrmann J, Rakhit A, Paul DL, Berul CI (2000) A targeted disruption in connexin40 leads to distinct AV conduction defects. J Interv Card Electrophys 4: 459–467
9. Bigger JT, Fleiss JL, Rolnitzky LM, Steinman RC (1993) The ability of several short-term measures of RR variability to predict mortality after myocardial infarction. Circulation 88: 927–934
10. Bigger JT, Fleiss JL, Steinman RC, Rolnitzky LM, Kleiger RE, Rottman JM (1992) Frequency domain measures of heart period variability and mortality after myocardial infarction. Circulation 85: 161–171
11. Cabo C, Schmitt H , Masters G, Coromilas J, Wit AL, Scheinman MM (1998) Location of diastolic potentials in reentrant circuits causing sustained ventricular tachycardia in the infarcted canine heart. Circulation 98: 2598–2607
12. Cerutti C, Gustin MP, Paultre CZ, Lo M, Julien C, Vincent M, Sassard J (1991) Autonomic nervous system and cardiovascular variability in rats. Am J Physiol 261: H1292–H1299
13. Chiou CW, Zipes DP (1998) Selective vagal denervation of the atria eliminates heart rate variability and baroreflex sensitivity while preserving ventricular innervation. Circulation 98: 360–368
14. Coleman TG (1980) Arterial baroreflex control of heart rate in the conscious rat. Am J Physiol 238: H515–H520
15. Cooley RL, Montano N, Cogliati C, van de Borne P, Richenbacher W, Oren R, Somers VK (1998) Evidence for a central origin of the low-frequency oscillation in RR-interval variability. Circulation 98: 556–561

16. Desai KH, Sato R, Schauble E, Barsh GS, Kobilka BK, Bernstein D (1997) Cardiovascular indexes in the mouse at rest and with exercise. Am J Physiol 272: H1053–H1061
17. Dillon SM, Allessie MA, Ursell PC, Wit AL (1988) Influences of anisotropic tissue structure in reentrant circuits in the epicardial border zone of subacute canine infarcts. Circ Res 63: 182–206
18. Doevendans PA, Daemen MJ, de Nunick ED, Smits JF (1998) Cardiovascular phenotyping in mice. Cardiovasc Res 39: 34–49
19. Eldar MD, Ohad A, Bor N, Swanson DK, Battler A (1994) A closed-chest pig model of sustained ventricular tachycardia. Pacing Clin Electrophysiol 17: 1603–1609
20. Farrell TG, Odemuyiwa O, Bashir Y, Cripps TR, Malik M, Ward DE, Camm AJ (1992) Prognostic value of baroreflex sensitivity testing after acute myocardial infarction. Br Heart J 67: 129–137
21. Fletcher PJ, Pfeffer JM, Pfeffer MA, Braunwald E (1981) Left ventricular diastolic pressure-volume relations in rats with healed myocardial infarction. Circ Res 49: 618–626
22. Gao XM, Dart AM, Dewar E, Jennings G, Du XJ (2000) Serial echocardiographic assessment of left ventricular dimensions and function after myocardial infarction in mice. Cardiovasc Res 45: 330–338
23. Garrey WE (1914) The nature of fibrillatory contraction of the heart: its relation to tissue mass and form. Am J Physiol 33: 397–414
24. Gehrmann J, Berul CI (2000) Cardiac electrophysiology in genetically engineered mice. J Cardiovasc Electrophysiol 11: 354–368
25. Gehrmann J, Hammer PE, Maguire CT, Wakimoto H, Triedman JK, Berul CI (2000) Phenotypic screening for heart rate variability in the mouse. Am J Physiol 279: H733–740
26. Guerrero PA, Schuessler RB, Lloyd MD, Beyer EC, Johnson CM, Yamada KA, Saffitz JE (1997) Slow ventricular conduction in mice heterozygous for a connexin43 null mutation. J Clin Invest 99: 1991–98
27. Hein L, Barsch GS, Pratt RE, Dzau VJ, Kobilka BK (1995) Behavioral and cardiovascular effects of disrupting the angiotensin II type-2 receptor gene in mice. Nature 377: 744–747
28. Hoit BD, Khan ZU, Pawloski-Dahm CM, Walsh RA (1997) In vivo determination of left ventricular shortening and wall stress relationship in normal mice. Am J Physiol 272: H1047–H1052
29. Houle MS, Billman GE (1999) Low-frequency component of the heart rate variability spectrum: a poor marker of sympathetic activity. Am J Physiol 276: H215–H223
30. Huang XD, Sandusky GE, Zipes DP (1999) Heterogeneous loss of connexin43 protein in ischemic dog hearts. J Cardiovasc Electrophysiol 10: 79–91
31. Hutter JJ, Mestril R, Tam EK, Sievers RE, Dillmann WH, Wolfe CL (1996) Overexpression of heatshock protein 72 in transgenic mice decreases infarct size in vivo. Circulation 94: 1408–1411
32. Ichiki T, Labosky PA, Shiota C, Fogo A, Nimura F, Ichikawa I, Hogan BL, Inagami T (1995) Effects on blood pressure and exploratory behavior of mice lacking angiotensin II type-2 receptor. Nature 377: 748–750
33. Ito M, Oliverio MI, Mannon PJ, Best CF, Maeda N, Smithies O, Coffman TM (1995) Regulation of blood pressure by the type 1A angiotensin II receptor gene. Proc Natl Acad Sci USA 92: 3521–3525
34. James JF, Hewett TE, Robbins J (1998) Cardiac physiology in transgenic mice. Circ Res 82: 407–415
35. Janse MJ, Kleber AG (1981) Electrophysiological changes and ventricular arrhythmias in the early phase of regional myocardial ischemia. Circ Res 49: 1069–1081
36. Janse MJ, Opthof T, Kleber AG (1998) Animal models of cardiac arrhythmias. Cardiovasc Res 39: 165–177
37. Jose AD (1966) Effect of combined sympathetic and parasympathetic blockade on heart rate and cardiac function in man. Am J Cardiol 18: 476–478
38. Jumrussirikul P, Dinerman J, Dawson TM, Dawson VL, Ekelund U, Schramm LP, Calkins H, Snyder SH, Hare JM, Berger RD (1998) Interaction between neuronal nitric oxide synthase and inhibitory G protein activity in heart rate regulation in conscious mice. J Clin Invest 102: 1279–1285
39. Kleiger RE, Miller JP, Bigger JT, Moss AJ (1987) Decreased heart rate variability and its association with increased mortality after acute myocardial infarction. Am J Cardiol 59: 256–262
40. Koch WJ, Rockman HA, Samama P, Hamilton RA, Bond RA, Milano CA, Lefkowitz RJ (1995) Cardiac function in mice overexpressing the β-adrenergic receptor kinase or a βARK inhibitor. Science 268: 1350–1352
41. Krueger C, Kalenka A, Haunstetter A, Schweizer M, Maier C, Ruhle U, Ehmke H, Kubler W, Haass M (1997) Baroreflex sensitivity and heart rate variability in conscious rats with myocardial infarction. Am J Physiol 273: H2240–H2247
42. Kumashiro H, Kusachi S, Moritani H, Ohnishi H, Nakahama M, Uesugi T, Ayada Y, Nunoyama H, Tsuji T (1999) Establishment of a long-surviving murine model of myocardial infarction: qualitative and quantitative conventional microscopic findings during pathological evolution. Basic Res Cardiol 94: 78–84
43. Kuwahara M, Yayou K, Ishii K, Hashimoto S, Tsubone H, Sugano S (1999) Power spectral analysis of heart rate variability as a new method for assessing autonomic activity in the rat. J Electrocardiol 32: 167–171
44. Lombardi F, Sandrone G, Pernpruner S, Sala R, Cerutti S, Baselli G, Pagani M, Malliani A (1987) Heart rate variability as an index of sympathovagal interaction after acute myocardial infarction. Am J Cardiol 60: 1239–1245
45. Luke RA, Saffitz JE (1991) Remodeling of ventricular conduction pathway in healed canine infarct border zones. J Clin Invest 87: 1594–1602
46. Lutgens E, Daemen MJM, de Muinck ED, Debets J, Leenders P, Smits JFM (1999) Chronic myocardial infarction in the mouse: cardiac structural and functional changes. Cardiovasc Res 41: 586–593
47. Malik M, Farrell T, Camm AJ (1990) Circadian rhythm of heart rate variability after acute myocardial infarction and its influence on the prognostic value of heart rate variability. Am J Cardiol 66: 1049–54
48. Malik M, Camm AJ (1990) Significance of long-term components of heart rate variability for further prognosis after acute myocardial infarction. Cardiovasc Res 24: 793–803
49. Malliani A, Pagani M, Lombardi F, Cerutti S (1991) Cardiovascular neural regulation explored in the frequency domain. Circulation 84: 482–492
50. Malliani A, Pagani M, Montano N, Mela GS (1998) Sympathovagal balance: a reappraisal. Circulation 98: 2640–2643
51. Manning WJ, Wei JY, Katz SE, Douglas PS, Gwathemy JK (1993) Echocardiographically detected myocardial infarction in the mouse. Lab Animal Sci 43: 583–585
52. Mansier P, Medigue C, Charlotte N, Vermeiren C, Coraboeuf E, Ratner E, Chevalier B, Carre F, Dahkli T, Bertin B, Strosberg D, Swynghedauw B (1996) Decreased heart rate variability in transgenic mice overexpressing atrial β_1-adrenoreceptors. Am J Physiol 271: H1465–H1472
53. Michael LH, Entman ML, Hartley CJ, Youker KA, Zhu J, Hall SR, Hawkins HK, Berens K, Ballantyne CM (1995) Myocardial ischemia and reperfusion: a murine model. Am J Physiol 269: H2147–2154
54. Milano CA, Allen LF, Rockman HA, Dolber PC, McMinn TR, Chien KR, Johnson TD, Bond RA, Lefkowitz RJ (1994) Enhanced myocardial function in transgenic mice overexpressing the β_2-adrenergic receptor. Science 264: 582–585
55. Mitchell GF, Jeron A, Koren G (1998) Measurement of heart rate and Q-T interval in the conscious mouse. Am J Physiol 274: H747–H751

56. Montano N, Ruscone TG, Porta A, Lombardi F, Pagani M, Malliani A (1994) Power spectrum analysis of heart rate variability to assess the changes in sympathovagal balance during graded orthostatic tilt. Circulation 90: 1826–1831
57. Morley GE, Vaidya D, Samie FH, Lo C, Delmar M, Jalife J (2000) Characterization of conduction in the ventricles of normal and heterozygous Cx43 knockout mice using optical mapping. J Cardiovasc Electrophysiol 11: 375–377
58. Odemuyiwa O, Malik M, Farrell T, Bashir Y, Poloniekci J, Camm AJ (1991) Comparison of the predictive characteristics of heart rate variability index and left ventricular ejection fraction for all-cause mortality, arrhythmic events and sudden death after acute myocardial infarction. Am J Cardiol 68: 434–439
59. Pagani M, Lombardi F, Guzzetti S, Rimoldi O, Furlan R, Sandrone G, Dell' Orto S, Tureil M, Basseli G, Cerutti S, Malliani A (1986) Power spectral analysis of heart rate and arterial pressure variabilities as a marker of sympatho-vagal interaction in man and conscious dog. Circ Res 59: 178–193
60. Pagani M, Mazzuero G, Ferrari A, Liberati D, Cerutti SY, Vaitl D, Tavazzi L, Malliani A (1991) Sympathovagal interaction during mental stress. Circulation 83: 43–51
61. Pattten RD, Aronovitz MJ, Deras-Meja L, Pandian NG, Hanak GG, Smith JJ, Mendelsohn ME, Konstam MA (1998) Ventricular remodeling in a mouse model of myocardial infarction. Am J Physiol 274: H1812–1820
62. Peters NS, Coromilas J, Severs NJ, Wit AL (1997) Disturbed connexin43 gap junction distribution correlates with the location of reentrant circuits in the epicardial border zone of healing canine infarcts that cause ventricular tachycardia. Circulation 95: 988–996
63. Pfeffer MA, Braunwald E (1990) Ventricular remodeling after myocardial infarction in rats. Circulation 81: 1161–1171
64. Priori SG, Barhanin J, Hauer RN, Haverkamp W, Jongsma HJ, Kleber AG, McKenna WJ, Roden DM, Rudy Y, Schwartz K, Schwartz PJ, Towbin JA, Wilde AM (1999) Genetic and molecular bases of cardiac arrhythmias: impact on clinical management Parts I and II. Circulation 99: 518–528
65. Pye MP, Cobbe SM (1996) Arrhythmogenesis in experimental models of heart failure: the role of increased load. Cardiovasc Res 32: 248–257
66. Qin D, Zhang ZH, Caref EB, Boutjdir M, Jain P, el-Sherif N (1996) Cellular and ionic basis of arrhythmias in postinfarction remodeled ventricular myocardium. Circ Res 79: 461–473
67. Reaume AG, deSousa PA, Kulkarni S, Langville BL, Zhu D, Davies TC, Juenja SC, Kidder GM, Rossant J (1995) Cardiac malformation in neonatal mice lacking connexin43. Science 267: 1831–1834
68. Rimoldi O, Pierini S, Ferrai A, Cerutti S, Pagani M, Malliani A (1990) Analysis of short-term oscillations of R-R and arterial pressure in conscious dogs. Am J Physiol 258: H967–H976
69. Rioufol G, Ovize M, Loufoua J, Pop C, Andre-Fouat X, Minaire Y (1997) Ventricular fibrillation in preconditioned pig hearts: role of K+ATP channels. Am J Physiol 273: H2804–H2810
70. Rodrigues TR, Miranda RC, Lichter AP, Lobo NC, Figueroa CS, Moreira MD (1996) Heart rate variability in myocardial infarction with and without maligant arrhythmias. Pacing Clin Electrophysiol 19: 1857–1862
71. Rohde LE, Ducharme A, Arroyo LH, Aikawa M, Sukhova GH, Lopez-Anaya A, McClure KF, Mitchell PG, Libby P, Lee RT (1999) Matrix metalloproteinase inhibition attenuates early left ventricular enlargement after experimental myocardial infarction in mice. Circulation 99: 3063–3070
72. Schwartz PJ, La Rovere MT, Vanoli E (1992) Autonomic nervous system and sudden cardiac death. Experimental basis and clinical observations for post-myocardial infarction risk stratification. Circulation 85 (1 Suppl): I77–91
73. Skyschally A, Breuer HM, Heusch G (1996) The analysis of heart rate variability does not provide a reliable measurement of cardiac sympathetic activity. Clin Sci 91: 102–104
74. Smith JH, Green CR, Peters NS, Rothery S, Severs NJ (1991) Altered patterns of gap junction distribution in ischemic heart disease. Am J Pathol 139: 801–821
75. Spear JF, Michelson EL, Moore EN (1982) The use of animal models in the study of the electrophysiology of sudden coronary deaths. Ann NY Acad Sci 382: 78–89
76. Sumeray MS, Rees DD, Yellon DM (2000) Infarct size and nitric oxide synthase in murine myocardium. J Mol Cell Cardiol 32: 35–42
77. Tanaka N, Dalton N, Lao L, Rockman HA, Peterson KL, Gottschal KR, Hunter JJ, Chien KR, Ross J (1996) Transthoracic echocardiography in models of cardiac disease in the mouse. Circulation 94: 1109–1117
78. Task Force of the European Society of Cardiology and the North American Society of Pacing and Electrophysiology (1996) Heart rate variability: standards of measurement, physiological interpretation, and clinical use. Circulation 93: 1043–1065
79. Uechi M, Asai K, Osaka M, Smith A, Sao N, Wagner TE, Ishikawa Y, Hayakawa H, Vatner DE, Shannon RP, Homcy CJ, Vatner SF (1998) Depressed heart rate variability and arterial baroreflex in conscious transgenic mice with overexpression of cardiac $G_{s\alpha}$. Circ Res 82: 416–423
80. Wickman K, Nemec J, Gendler SJ, Clapham DE (1998) Abnormal heart rate regulation in GIRK4 knockout mice. Neuron 20: 103–114
81. Yoshida T, Maulik N, Engelman RM, Ho YS, Das DK (2000) Targeted disruption of the mouse Sod I gene makes the heart vulnerable to ischemic reperfusion injury. Circ Res 86: 264–269
82. Zipes DP (1990) Influence of myocardial ischemia and infarction on autonomic innervation of heart. Circulation 82: 1095–1105
83. Zolotareva AG, Kogan ME (1978) Production of experimental occlusive myocardial infarction in mice. Cor Vasa 20: 308–314